Collective excitations in liquid ^{4}He. II. Analysis and comparison with theory

1994 J. Phys.: Condens. Matter 6 5805

(http://iopscience.iop.org/0953-8984/6/30/004)

J. Phys.: Condens. Matter 6 (1994) 5805–5822. Printed in the UK

Collective excitations in liquid ^{4}He: II. Analysis and comparison with theory

K H Andersen†‡§ and W G Stirling‡

† Institut Laue–Langevin, BP 156X, 38042 Grenoble Cédex, France

‡ Department of Physics, School of Science and Engineering, Keele University, Keele, Staffordshire, ST5 5BG, UK

Received 25 October 1993, in final form 9 May 1994

Abstract. In a previous paper neutron inelastic scattering results were presented on the temperature dependence of the excitation spectrum of liquid ^{4}He in the phonon–roton region. This paper discusses these results in the light of different theoretical analysis procedures, namely the Woods–Svensson hypothesis, the multiphonon subtraction due to Miller *et al*, and the new Glyde–Griffin theory. The Woods–Svensson hypothesis that the scattering can be decomposed into normal and superfluid parts is examined in detail, but is found to be too simple to accurately describe the observed temperature dependence. This model is used, however, to extract one-phonon parameters, as is the simple multiphonon subtraction model. The data of Andersen *et al* show that $S(Q,\omega)$ does indeed change character at or just below T_λ, the effect being particularly marked at the larger wavevectors considered. This behaviour is in agreement with a recent interpretation by Glyde and Griffin, in which the rotons are seen as single-particle excitations, coupled to the density fluctuations through the presence of a finite Bose condensate. The abrupt disappearance from the density fluctuation spectrum of this mode of excitation at T_λ gives rise to a sudden change in $S(Q,\omega)$. A parametrization of the Glyde–Griffin model is compared with the data and provides qualitative agreement with the observed temperature dependence.

1. Introduction

The phonon–roton excitations of superfluid ^{4}He and the higher-energy multiphonon continuum have been studied continuously by neutron scattering techniques since the pioneering observations of roton scattering by Palevsky *et al* (1957), but there are still fundamental uncertainties as to the nature of these excitations. Recent work has concentrated on the temperature dependence and the microscopic origin of these uniquely 'sharp' excitations. An excellent detailed review of work up to 1987 is given by Glyde and Svensson (1987). In the previous paper of this series (Andersen *et al* 1994, hereafter referred to as paper I) we reported neutron (time of flight) inelastic scattering measurements of the excitation spectrum of ^{4}He in both superfluid and normal fluid phases. The range in wavevector from 0.3 to 2.1 Å^{-1} was investigated for excitation energies up to about 3.5 meV. Measurements were made of the scattering function $S(Q,\omega)$ at 15 temperatures between 1.24 K and 4.95 K at saturated vapour pressure (SVP). Preliminary reports of this work have been published elsewhere (Stirling 1991, Andersen *et al* 1992). The results of these experiments are given in paper I and are exemplified by the data presented in figure 9.

§ Current address: Booster Synchrotron Utilization Facility, National Laboratory for High-Energy Physics, 1-1 Oho, Tsukuba-shi, Ibaraki-ken, 305 Japan.

0953-8984/94/305805+18$19.50

As seen in previous more limited experiments (Woods and Svensson 1978, Talbot *et al* 1988, Stirling and Glyde 1990) the excitations were found to change much more rapidly in the superfluid phase below the lambda point at $T_\lambda = 2.17$ K than in the normal fluid phase. Furthermore, there is a marked difference between 'small' ($Q <\sim 0.8$ Å^{-1}) and 'large' wavevectors; in the former case a broadened peak persists at essentially the same energy above the lambda point whereas in the latter case the much weaker, very wide response is peaked at a significantly different energy.

Analysis of the data is complicated by the existence of both single-phonon and multiphonon scattering and by the fact that there is no microscopically based theory detailed enough to allow a quantitative comparison with the measured $S(Q,\omega)$ as a function of temperature. A basic theory does exist, describing the expected temperature dependence of the one-phonon peak in the roton region (Landau and Khalatnikov 1949, Bedell *et al* 1984), which suggests that a decomposition of the total $S(Q,\omega)$ into one-phonon and other contributions may be useful. The temperature dependence of the one-phonon lineshape can then more easily be parametrized and compared with theory. We emphasize that many of the inconsistencies between phonon parameters (energy, width/lifetime, strength) in the literature result from inadequacies in the analysis procedures. One of our aims in this work has been to provide reliable one-phonon parameters using carefully defined and objective criteria. We have considered two procedures aimed at extracting the one-phonon component of $S(Q,\omega)$.

The first is a method proposed by Woods and Svensson (1978). In the Woods–Svensson (WS) decomposition, the total $S(Q,\omega)$ is taken to consist of three parts: the one-phonon component, which is assumed to scale as the hydrodynamic superfluid density ρ_S, a multiphonon component, also scaling as ρ_S, and a normal fluid component, which scales as ρ_N, the normal fluid density. The form of this decomposition was suggested by the observed temperature dependence of $S(Q,\omega)$, and does not have any theoretical basis. The WS superfluid component was shown to exhibit a much simpler temperature dependence than the combined $S(Q,\omega)$ and parameters extracted from the separated WS one-phonon peaks were in better agreement with calculated one-phonon properties than values extracted from the total $S(Q,\omega)$. The WS procedure describes the observed temperature dependence at SVP reasonably well. There are thus two reasons for performing an analysis in terms of the WS procedure. One is that we desire an objective procedure to extract the one-phonon peak from the measured data and the other is that we are now able to perform a significantly more stringent test of WS than has previously been possible.

The second method we use to extract the one-phonon component is the simple multiphonon subtraction (SS) of Miller *et al* (1962), in which the total $S(Q,\omega)$ at all temperatures is taken to consist of the sum of a one-phonon and a multiphonon part. For simplicity, the multiphonon component is assumed to be independent of temperature, such that all of the temperature dependence is contained in the one-phonon peak. Whilst the detailed shape of the multiphonon scattering is not expected to be independent of temperature, the procedure is still useful in allowing us a second method for extracting a one-phonon component from $S(Q,\omega)$. In particular, since the SS procedure defines a one-phonon peak at all temperatures, we can use it to look at the behaviour of $S(Q,\omega)$ at the λ transition, to see whether an abrupt change occurs when entering the superfluid phase.

In addition to the above analyses of the one-phonon peak, we also consider a recent theory describing the temperature dependence of the total $S(Q,\omega)$. This is the model proposed by Glyde and Griffin (GG) (1990). The GG scenario is complete in that it provides a consistent microscopic basis for a description of the total $S(Q,\omega)$ at all temperatures and all wavevectors in the collective excitation regime. There is no parametrization of GG

available, however, that will allow a quantitative comparison with the data. In the present paper, we make qualitative comparisons with the parametrization suggested by Glyde (1992), in which the parameters are defined by consideration of neutron scattering data.

The paper is laid out as follows. Section 2 describes the one-phonon lineshape employed and the instrumental resolution function used in the following analyses. Sections 3, 4, and 5 discuss the present results in the light of the WS decomposition and the SS procedure, which are used to determine the one-phonon parameters (position, width, strength). Section 6 deals with the GG model, with discussion and conclusions following in section 7.

2. Lineshape and instrumental resolution analysis

To describe the temperature variation of the sharp peak in $S(Q,\omega)$ a quantitative analysis of the peak position, width, and strength is required, taking account of the instrumental resolution function. We fit the sharp peak to the conventional damped harmonic oscillator (DHO) function (Talbot *et al* 1988, Dorner 1992):

$$S_1(Q,\omega) = (Z_Q/\pi)[n_B(\omega)+1][\Gamma_Q/[(\omega-\omega_Q)^2+\Gamma_Q^2] - \Gamma_Q/[(\omega+\omega_Q)^2+\Gamma_Q^2]] \quad (1)$$

$$= (Z_Q/\pi)[n_B(\omega)+1]4\omega\omega_Q\Gamma_Q/\{[\omega^2-(\omega_Q^2+\Gamma_Q^2)]^2+[2\omega\Gamma_Q]^2\} \quad (2)$$

where Z_Q is an intensity normalization factor, Γ_Q is the half width at half maximum (HWHM), ω_Q is the excitation energy, and $n_B(\omega)$ is the Bose factor. From equations (1) and (2) it can be seen that the 'double-Lorentzian' form of equation (1) is mathematically identical to the DHO function of equation (2). To extract the one-phonon parameters Z_Q, ω_Q and Γ_Q, we need a detailed description of the instrumental resolution lineshape, which can best be obtained from the low-temperature data. Mezei and Stirling (1983) have measured the one-phonon width with very high resolution as a function of Q, using triple-axis and neutron spin echo (NSE) techniques. They find that at a temperature of 1.2 K, the width (FWHM) of the one-phonon peak is approximately 7 μeV and is largely independent of Q. At $T = 1.3$ K the one-phonon peaks in the present experiment are well separated from the much weaker multiphonon scattering (figure 3 of paper I) and have widths (FWHM) of about 100 μeV, much larger than the 'physical' widths determined by Mezei and Stirling. Thus the present low-temperature data ($T = 1.24$ K and $T = 1.30$ K) are dominated by instrumental resolution effects. The very high statistical precision of the data allows a detailed analysis of the one-phonon peak shape; a Gaussian model for the instrumental resolution function was found to be inadequate and to give too little intensity in the wings of the peak. Consequently, an alternative resolution function was constructed, consisting of a Gaussian function plus a Lorentzian function in linear superposition:

$$R(Q,\omega) = (Z_{res}/\pi)\Gamma_{res}/(\omega^2+\Gamma_{res}^2) + \left\{[1-Z_{res}]/\sqrt{2\pi\sigma_{res}^2}\right\}\exp(-\omega^2/2\sigma_{res}^2). \quad (3)$$

A resolution lineshape with non-Gaussian wings has previously been observed for the IN6 instrument (Marshall 1994). The resolution function parameters Z_{res}, Γ_{res} and σ_{res} were determined at each wavevector by performing a least-squares fit to the DHO peak shape (equations (1) and (2)) convoluted with the above resolution function. The half width Γ_Q of the intrinsic DHO peak was fixed at the value determined by Mezei and Stirling (1983) and the three resolution function parameters, along with Z_Q and ω_Q, were allowed to vary freely. To avoid complications due to the multiphonon scattering at energies above ω_Q the fits were preferentially weighted to the low-energy side of the one-phonon peak. Typical fitted values of the resolution parameters are, for $Q = 1.00$ Å^{-1}, $Z_{res} = 0.05$, $\Gamma_{res} = 0.15$ meV, and $\sigma_{res} = 0.04$ meV.

3. The Woods–Svensson decomposition

The form of the decomposition proposed by WS (1978) into superfluid (S_S) and normal fluid (S_N) parts can be written as

$$S(Q,\omega;T) = (\rho_S/\rho)(T)S_S(Q,\omega;T) + (\rho_N/\rho)(T)S_N(Q,\omega;T) \tag{4}$$

where ρ_N is the normal fluid density, ρ_S is the superfluid density, and $\rho = \rho_N + \rho_S$ is the total density of the fluid. The temperature dependence of S_N is assumed to be entirely due to the Bose factor with

$$S_N(Q,\omega;T) = -(1/\pi)[n_B(\omega;T)+1]\,\mathrm{Im}\,\chi_N(Q,\omega). \tag{5}$$

At temperatures just above T_λ, the imaginary part of the dynamic susceptibility is taken to be independent of temperature, and S_N is determined by measuring $S(Q,\omega)$ at a temperature $T_{\lambda+} = 2.26$ K:

$$S_N(Q,\omega;T) \equiv [(1-\mathrm{e}^{-\hbar\omega/k_BT_{\lambda+}})/(1-\mathrm{e}^{-\hbar\omega/k_BT})]S(Q,\omega;T_{\lambda+}). \tag{6}$$

The 'superfluid' component of $S(Q,\omega)$ is found by subtracting the normal fluid term from the measured $S(Q,\omega)$ and is seen to consist of a sharp component S_1^{WS} and a multiphonon 'background' S_m^{WS}:

$$(\rho_S/\rho)(T)S_S(Q,\omega;T) = S_1^{WS}(Q,\omega;T) + (\rho_S/\rho)(T)S_m^{WS}(Q,\omega) \tag{7}$$

where the multiphonon component S_m^{WS} is assumed to be independent of temperature. S_m^{WS} can be obtained by subtracting the normal fluid component and the one-phonon peak from the observed scattering at the lowest measured temperature $T_{min} = 1.24$ K:

$$\begin{aligned} &S_m^{WS}(Q,\omega) \equiv 0 \qquad \text{if } \omega < \omega_Q \\ &S_m^{WS}(Q,\omega) \equiv (\rho/\rho_S)(T_{min})[S(Q,\omega;T_{min}) - S_1(Q,\omega;T_{min}) \\ &\qquad - (\rho_N/\rho)(T_{min})S_N(Q,\omega;T_{min})] \qquad \text{if } \omega > \omega_Q \end{aligned} \tag{8}$$

where S_1 of equation (8) is defined to be the DHO function (equations (1) and (2)) with a width given by the Mezei and Stirling (1983) measurement, convoluted by the instrumental resolution function (equation (3)). S_m^{WS} is not corrected for the temperature dependence of the detailed balance factor, as this is only important at low energies, and the multiphonon continuum starts at energies above the one-phonon peak, as ensured by the form of equation (8).

The one-phonon peak, as defined by WS, is then obtained by subtracting the normal fluid and multiphonon components from the observed scattering at $T < T_\lambda$:

$$S_1^{WS}(Q,\omega;T) \equiv S(Q,\omega;T) - [(\rho_N/\rho)(T)S_N(Q,\omega;T) + (\rho_S/\rho)(T)S_m^{WS}(Q,\omega;T)]. \tag{9}$$

At $T > T_\lambda$ there is no WS one-phonon peak defined. The WS decomposition was performed at all measured wavevectors at the eight measured temperatures up to and including T_λ and the DHO lineshape convoluted by the resolution function was fitted to the resulting $S_1^{WS}(Q,\omega;T)$ for extraction of the one-phonon parameters. Figure 1 shows the WS decomposition of our data at $Q = 0.40$ Å^{-1} (phonon region), $Q = 1.10$ Å^{-1} (maxon region), and $Q = 1.95$ Å^{-1}

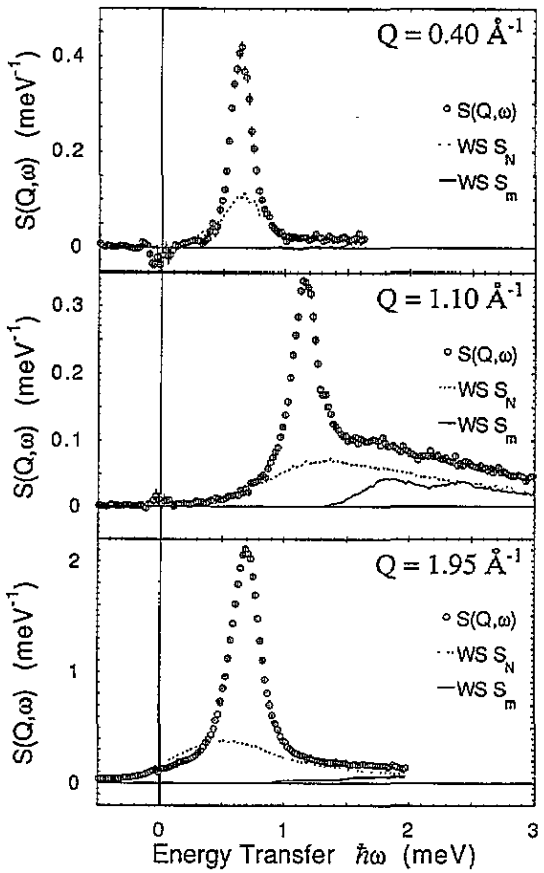

Figure 1. Examples of the WS decomposition of the observed $S(Q,\omega)$ at $T = 1.96$ K for $Q = 0.40$ Å^{-1}, $Q = 1.10$ Å^{-1}, and $Q = 1.95$ Å^{-1}. The experimental data are shown by the open circles, the normal fluid component $(\rho_N/\rho)S_N$ by the dotted curve, and the multiphonon component $(\rho_S/\rho)S_m^{WS}$ by the full curve.

(roton region) at a temperature of 1.96 K. The normal fluid component $(\rho_N/\rho)S_N$ and the multiphonon component $(\rho_S/\rho)S_m^{WS}$ are shown by dotted and full curves respectively. Figure 2 presents the WS one-phonon excitation lineshapes derived in this way for the representative wavevectors, $Q = 0.40$ Å^{-1}, 1.10 Å^{-1}, and 1.95 Å^{-1}.

With the data available at the time, WS showed that $S(Q,\omega)$ of liquid ^{4}He at SVP apparently separated naturally into a normal and a superfluid component. However, Talbot *et al* (1988) have examined the temperature dependence of $S(Q,\omega)$ at a pressure of 20 bars, and they found that such a separation is not physically meaningful, as it resulted in oversubtractions such that S_1^{WS} took negative values at low ω. The data of Andersen *et al* (1994) combine high resolution with good statistical precision, allowing an even more stringent test of the WS decomposition at SVP than in the original WS paper. Figure 3 presents a magnified view of the low-energy wing of the WS one-phonon peak (S_1^{WS}) at the roton wavevector, and it is seen that a similar conclusion to that of Talbot *et al* can be reached from these data at SVP. The scattering intensity of S_1^{WS} is negative at low ω in the roton region, which is not physically meaningful, and it follows that too much intensity is subtracted if the normal fluid component is scaled as ρ_N/ρ. Examination of figure 2 shows

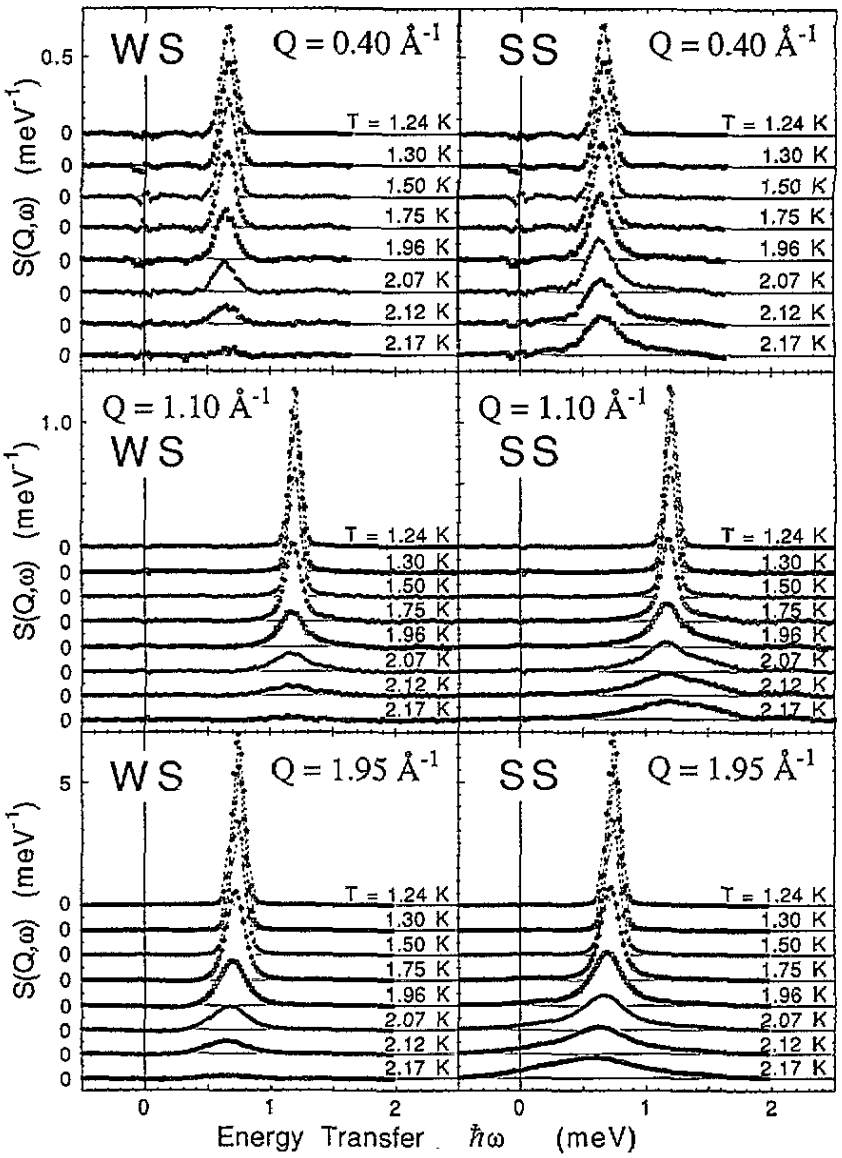

Figure 2. *Left panel: the temperature dependence of the* WS *one-phonon component* S_1^{WS} *for* $Q = 0.40$ Å^{-1}, $Q = 1.10$ Å^{-1}, and $Q = 1.95$ Å^{-1}. Note that this component only exists below T_λ. Right panel: the temperature dependence of the SS one-phonon component S_1^{SS} for $Q = 0.40$ Å^{-1}, $Q = 1.10$ Å^{-1}, and $Q = 1.95$ Å^{-1}. Note that this exists both below and above T_λ.

that a similar though smaller oversubtraction occurs at the phonon wavevector while S_1^{WS} does not exhibit this unphysical negative intensity in the maxon region. Apart from this feature of the model, the WS decomposition does provide a very reasonable representation of the temperature variation of the measured $S(Q, \omega)$.

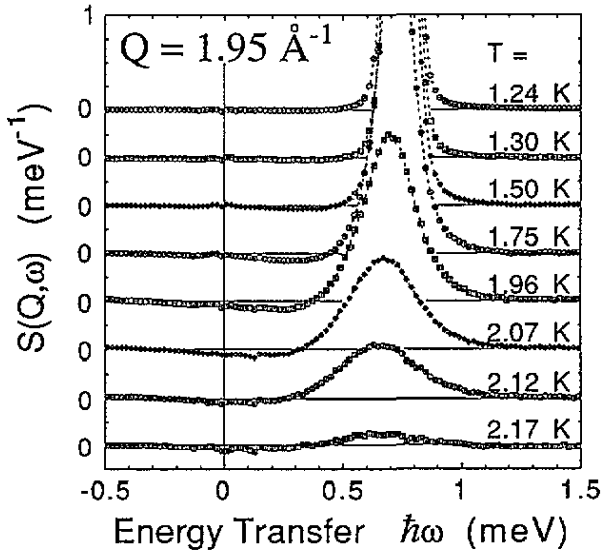

Figure 3. Expanded view of the one-phonon component $S_1^{WS}(Q,\omega)$ at the roton wavevector demonstrating the oversubtraction at low energies.

4. The simple multiphonon subtraction procedure

An alternative procedure for separating out the one-phonon peak was suggested by Miller *et al* (1962) and used by Cowley and Woods (1971) and also by Talbot *et al* (1988) in the analysis of data taken at 20 bars pressure. The total scattering is taken to consist of the sum of a single-phonon (S_1^{SS}) and a multiphonon component (S_m^{SS}), the latter of which is assumed to be independent of temperature, and is given by

$$S_m^{SS}(Q,\omega) \equiv S(Q,\omega;T_{min}) - S_1(Q,\omega;T_{min}). \tag{10}$$

That is, S_m^{SS} is taken to be the scattering measured at the lowest recorded temperature (T_{min} = 1.24 K) minus the sharp peak, which was found in the preceding section for extraction of the WS multiphonon spectrum (S_1 in equation (8)). The one-phonon peak is then found by a simple subtraction (SS) of the multiphonon spectrum:

$$S_1^{SS}(Q,\omega;T) \equiv S(Q,\omega;T) - S_m^{SS}(Q,\omega). \tag{11}$$

At $T = T_{min}$, equation (11) simply reproduces the lowest-temperature (T_{min}) one-phonon peak (which has the width given by the Mezei and Stirling (1983) measurements). Assuming the multiphonon component to be temperature independent is probably an oversimplification. In the limit of high ω, $S(Q,\omega)$ of liquid ^{4}He is indeed seen to be temperature independent, as confirmed by our measurements, but studies of quantum solids (Glyde and Svensson 1987) show that the two-phonon contribution to $S(Q,\omega)$ increases with T at low ω. We must expect some systematic errors to appear from neglecting the temperature dependence of the multiphonon component. However the SS procedure is still useful in that it defines a one-phonon peak at all temperatures without biasing it to show qualitative changes at T_λ.

Examples of the SS one-phonon peaks isolated as described above are presented in figure 2; the progressive broadening with increasing temperature is apparent, as is the continued existence of a one-phonon component at (and above) T_λ. These SS one-phonon components were fitted to the DHO function (equations (1) and (2)), convoluted with the resolution function of equation (3), with Z_Q, Γ_Q, and ω_Q as free parameters, as was done for the case of the WS one-phonon peak.

5. Evaluation of WS and SS results

Before proceeding to a consideration of the Glyde–Griffin (1990) model it is instructive to evaluate the present data as analysed above using the WS and SS procedures. Figure 4 presents the one-phonon peak widths $2\Gamma_Q$ obtained by the WS and SS methods, as a function of Q at various temperatures. The WS results are seen to be in reasonable agreement with the high-resolution measurements of Mezei (1980) and Mezei and Stirling (1983); agreement is less good for the SS results. For temperatures above 1.5 K, the widths are strongly Q dependent. Up to 1.5 K the two analysis methods produce widths that are very similar; above this temperature the values of $2\Gamma_Q$ differ increasingly, reflecting the basic differences between the two models. The present data suggest that at low Q (< 0.25 Å^{-1}), $S(Q,\omega)$ remains sharply peaked at all temperatures, though this is outside the range of the present measurements.

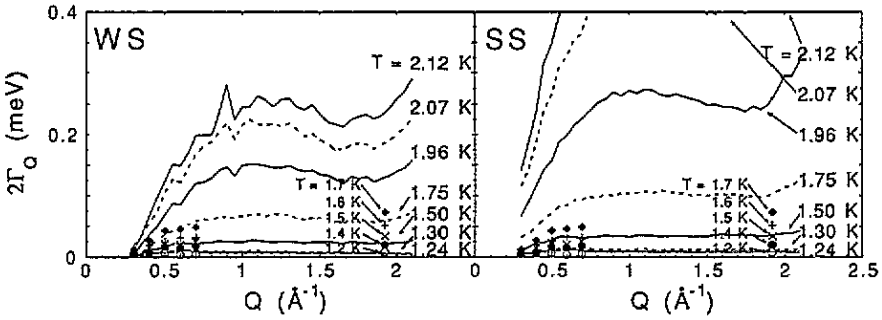

Figure 4. Left panel: the wavevector variation of the one-phonon widths $2\Gamma_Q(T)$ extracted using the WS method (full and dashed curves); for comparison the values obtained by Mezei (1980) and Mezei and Stirling (1983) are shown as the symbols. Right panel: as above for the SS method.

Figures 5–7 show the variation with temperature of the best-fit one-phonon parameters at three selected, representative wavevectors $Q = 0.40$, 1.10, and 1.95 Å^{-1}. In addition to the one-phonon parameters extracted using the WS and SS procedures, we also display the results of fitting the DHO lineshape to the *total* $S(Q,\omega)$ with no separation into one-phonon and other components. Figure 1 shows that, especially near T_λ, a single DHO function cannot describe well the *total* $S(Q,\omega)$. Hence the fit to the total $S(Q,\omega)$ was only performed at $T > T_\lambda$, where the lineshape of the data can be reasonably well described by a single DHO peak.

The normalization factor Z_Q in the DHO expression (equations (1) and (2)) is not in itself proportional to the peak intensity. A better measure of this is the area (or integral) of the best-fit DHO peak. This is shown in figure 5 as a function of temperature in the

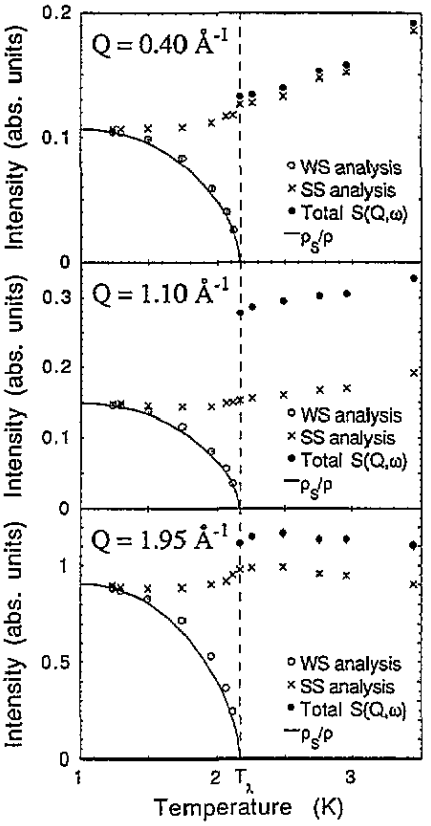

Figure 5. The one-phonon intensity, defined as the area of the best-fit DHO to the WS (open circles) and SS (crosses) models for wavevectors $Q = 0.40$ Å^{-1}, $Q = 1.10$ Å^{-1}, and $Q = 1.95$ Å^{-1}; the intensity integrated over energy is in units of $S(Q)$, i.e. dimensionless. The result of fitting to the total $S(Q, \omega)$ above T_λ is also shown (full circles). The full curve represents the ratio ρ_S/ρ, scaled to the WS result at $T_{min} = 1.24$ K. Error bars are given for all points, but are often smaller than the symbols.

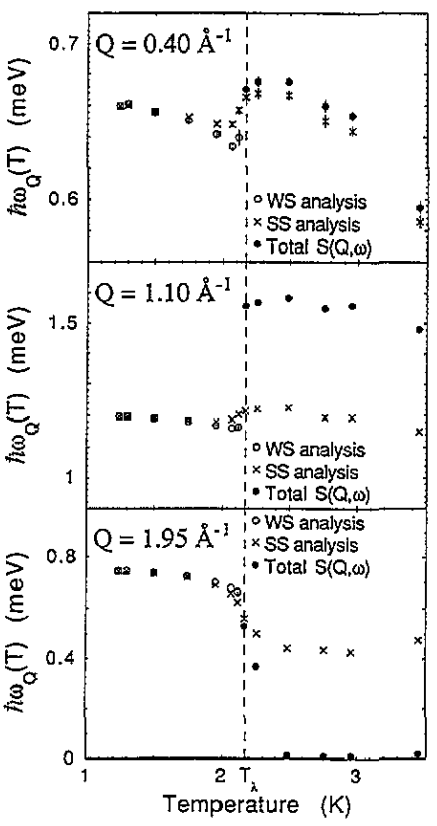

Figure 6. The one-phonon peak position $\hbar\omega_Q(T)$ extracted using the WS (open circles) and SS (crosses) methods, at the three representative wavevectors of figure 5. The peak position of the total $S(Q, \omega)$ is shown above T_λ (full circles). Error bars are as in figure 5.

phonon, maxon, and roton regions for both SS and WS procedures. The superfluid fraction (Maynard 1976) is also shown, scaled to agree with the WS single-phonon intensity at the lowest temperature $T_{min} = 1.24$ K. At first sight it appears that the WS one-phonon intensity scales very closely as ρ_S/ρ. This is somewhat misleading, however, as the scaling of S_1^{WS} is tightly constrained by its definition in equation (9). Minéev (1980) and Talbot *et al* (1988) have pointed out that S_1^{WS} as defined by WS *necessarily* scales as ρ_S/ρ if $S(Q)$ is approximately independent of T. This follows if the one-phonon peak intensity is defined as $S_1^{WS}(Q, \omega)$, integrated over all ω. Using the fact that the static structure factor $S(Q)$ is approximately temperature independent from $T = 1.0$ K to T_λ, they find that the intensity of the one-phonon peak must be proportional to ρ_S/ρ, by its definition in equation (9). In the present data analysis, the one-phonon intensity is not defined by the integrated intensity of the peak, but as the area of the best-fit DHO peak. Despite the forced scaling of the

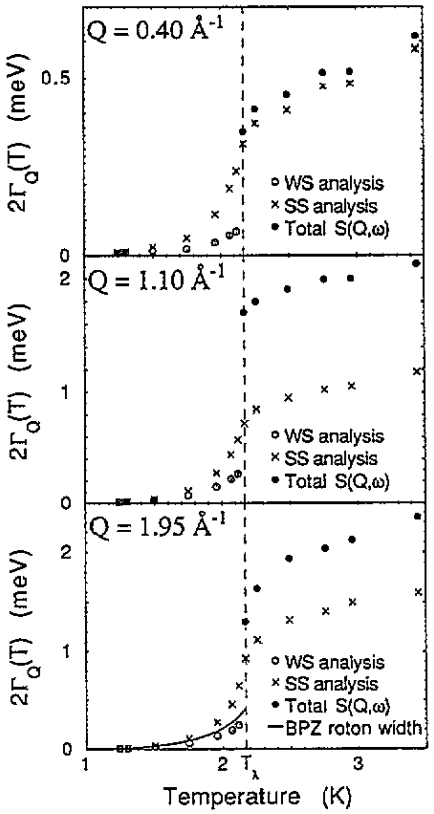

Figure 7. The one-phonon width $2\Gamma_Q(T)$ extracted using the WS (open circles) and SS (crosses) methods, at the three representative wavevectors of figure 5. The width of the total $S(Q,\omega)$ is shown above T_λ (full circles). For comparison the roton width calculated by Bedell, Pines, and Zawadowki (BPZ) (1984) is indicated by the full curve below T_λ. Error bars are as in figure 5.

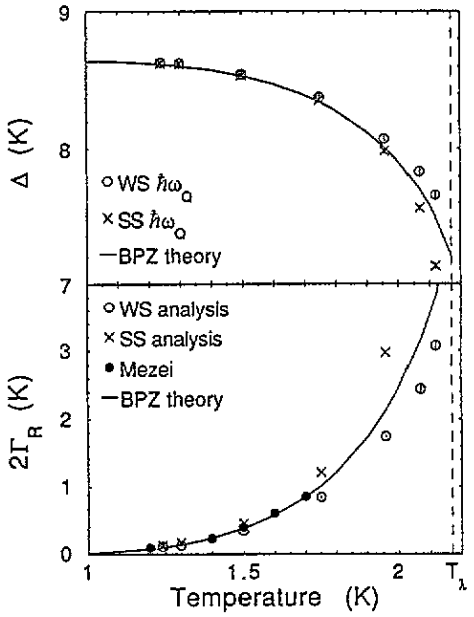

Figure 8. Upper panel: the temperature variation of the roton energy gap Δ as determined by the WS (open circles) and SS (crosses) methods. The calculation of BPZ (1984) is given by the full curve. Lower panel: the temperature variation of the roton width $2\Gamma_R$ as obtained by the WS (open circles) and SS (crosses) methods. The calculation of BPZ (1984) is given by the full curve and the Mezei (1980) values by the full circles. Error bars are as in figure 5.

one-phonon intensity, the temperature dependence of the extracted one-phonon intensity is seen in figure 5 to deviate systematically from that of ρ_S.

The SS separation differs from the WS procedure in that the single-phonon intensity is not forced to go to zero at T_λ. The one-phonon intensity of the SS model is seen to remain relatively constant with temperature, which is mainly a consequence of its definition. Since $S(Q)$ is approximately independent of T, S_1^{SS}, which is obtained by subtracting a temperature independent S_m^{SS}, must also be approximately independent of T. Figure 5 also demonstrates that the SS one-phonon intensity displays some change at T_λ at both the phonon and roton wavevectors, but seems unaffected by the λ transition in the maxon region.

Figure 6 displays the single-phonon energies $\hbar\omega_Q$ as a function of temperature, in the phonon, maxon, and roton regions. For temperatures up to 1.7 K the two models give almost exactly the same frequencies ω_Q. At all three wavevectors, the SS one-phonon energies are seen to change abruptly at T_λ. By examining the SS one-phonon parameters, we see that

even the low-Q (phonon) excitation changes character at the λ transition in much the same way as the maxon and roton excitations. The WS positions 'soften' somewhat as T_λ is approached; of course, there is no WS one-phonon peak above T_λ. We note the apparent 'collapse' of the roton frequency for the total $S(Q,\omega)$ above T_λ. This arises due to the very large roton width; at these temperatures the DHO is a convenient fitting function but the interpretation of ω_Q as a single excitation frequency is no longer meaningful. A similar effect was found by Stirling and Glyde (1990) who analysed their triple-axis spectrometer data using the DHO model of equation (1).

Calculating the roton decay rate by emission of phonons, Landau and Khalatnikov (1949) obtained an expression for the roton lifetime at low temperature. Bedell, Pines, and Zawadowski (BPZ) (1984) have extended this calculation to temperatures up to T_λ by including roton–roton interactions via a pseudopotential. BPZ have also calculated the temperature dependence of the roton energy gap, which can be obtained from the same roton decay mechanism. The excitation widths obtained from the present SS and WS one-phonon peaks in the phonon, maxon, and roton regions are shown in figure 7, along with the BPZ roton width predictions. The SS widths are seen to display a much stronger temperature dependence than those determined by the WS method. This is because more of the temperature dependent 'background' is subtracted in the WS procedure, leaving a narrower peak that changes less with temperature. The WS roton widths are seen to be close to but systematically smaller than the BPZ predictions, which may be due to the negative wings of the WS one-phonon peak S_1^{WS} at the roton wavevector. The DHO function cannot take negative values, and is instead biased towards a smaller width.

The roton energies and widths obtained by both the WS and SS methods are presented in figure 8, as a function of temperature, along with the NSE widths of Mezei (1980) and the BPZ calculations. Since the absolute values of the roton parameters are of fundamental importance for many thermodynamic properties (Woods *et al* 1977, Donnelly *et al* 1981) they have been determined directly from *constant-scattering-angle* data, to minimize errors introduced by the rebinning procedure; this is discussed further below. The WS and SS roton energies ($\hbar\omega_Q$) are seen to be close to but systematically slightly above the BPZ calculations for T above 1.7 K, while the SS energies are slightly below. The WS widths obtained from the present data are consistently lower for T above about 1.7 K than both the Mezei (1980) measurements and the BPZ theory, which are in excellent agreement. This can be attributed to the negative wings that appear in $S_1^{WS}(Q,\omega)$ at temperatures above 1.5 K, which bias the DHO function to smaller widths, as described above. The roton widths obtained by the SS method are about 50% greater than the WS widths, as less of the 'background' is subtracted. In general it is seen that the WS procedure gives values in better agreement with the BPZ calculations than the simple multiphonon subtraction. We note that above about 1.5 K the extracted widths depend sensitively on the method used for separating the single-phonon peak.

The roton parameters of figure 8 have been obtained by constant-scattering-angle fits to the WS and SS model one-phonon peaks. When performing the constant-Q rebinning, the width ΔQ of the required scan must be chosen to be substantially greater than the Q-width of the individual spectra, to minimize correlation effects. Using the data in its constant-scattering-angle format thus allows the parameter evaluations to be made at more positions in wavevector Q. The non-rebinned data have been used to fit a parabolic dispersion curve of the form

$$\hbar\omega(Q) = \hbar\omega_R + \hbar^2(Q - Q_R)^2/2\mu_R \tag{12}$$

to the ω_Q around the roton minimum, for each temperature. Table 1 lists the WS roton parameters Q_R, ω_R, and μ_R as a function of temperature, obtained from a least-squares fit

to equation (12). $2\Gamma_R(T)$ from the present data is also listed, obtained by an interpolation of $2\Gamma_Q$ at the roton wavevector Q_R. It is seen that Q_R is constant within error, which reflects the fact that the ^{4}He number density is constant to within 0.5% for $T < T_\lambda$. There is no need to correct for the effects of the Jacobian, which can be important when measuring along lines of constant scattering angle in the $(Q$–$\omega)$ plane, rather than constant Q, since the slope of the dispersion curve is zero at the roton wavevector.

Table 1. ws roton parameters.

T (K)	Q_R (Å^{-1})	$\hbar\omega_R$ (K)	μ_R (^{4}He mass)	$2\Gamma_R$ (K)
1.24	1.929 ± 0.003	8.625 ± 0.020	0.142 ± 0.003	0.11 ± 0.01
1.30	1.929 ± 0.003	8.619 ± 0.020	0.141 ± 0.003	0.13 ± 0.01
1.50	1.929 ± 0.003	8.538 ± 0.020	0.137 ± 0.003	0.34 ± 0.01
1.75	1.927 ± 0.003	8.371 ± 0.020	0.144 ± 0.004	0.84 ± 0.01
1.96	1.927 ± 0.003	8.072 ± 0.020	0.136 ± 0.004	1.74 ± 0.02
2.07	1.927 ± 0.003	7.832 ± 0.025	0.135 ± 0.003	2.44 ± 0.04
2.12	1.929 ± 0.003	7.660 ± 0.030	0.130 ± 0.008	3.07 ± 0.08

In conclusion, we find that it is not possible to extract model-independent parameters for the one-phonon peak above about 1.6 K. At higher temperatures, the sharp excitation is no longer well separated from the continuum scattering, and any decomposition of $S(Q,\omega)$ with the aim of separating out the sharp contribution must make implicit assumptions about its temperature dependence. The description of the one-phonon component also becomes increasingly ambiguous at higher temperatures. When the peak is broad, the one-phonon parameters ω_Q and Γ_Q are no longer independent of frequency and S_1 cannot be described in terms of a simple energy and lifetime. The DHO peak shape gives a good fit to the data for T below 1.6 K, whereas at higher temperature neither the SS nor the WS one-phonon lineshape is Lorentzian, and the parameters obtained must be viewed within the strict definition of each model.

6. The Glyde–Griffin formalism

The SS procedure is useful in that it defines a one-phonon peak at *all* temperatures, both below and above the lambda point; it is clear from figures 5, 6, and 7 that $S(Q,\omega)$ does change abruptly at T_λ over the entire measured wavevector range, which was not obvious at the phonon wavevector by simple visual inspection of the measured $S(Q,\omega)$ (figures 5–7 of paper I). An exciting recent theoretical development which accounts, at least qualitatively, for many of the features observed in this investigation (and in previous less complete studies) is that due to Glyde and Griffin (GG) (Glyde and Griffin 1990, Glyde 1992, Griffin 1993), which was developed from a consideration of high-resolution triple-axis measurements (Talbot *et al* 1988, Stirling and Glyde 1990). This model is an extension of the dielectric formulation of Bose fluids (Hugenholtz and Pines 1959, Gavoret and Nozieres 1964) and takes explicit account of the existence of a Bose condensate in the superfluid phase.

GG argue that the total dynamical susceptibility $\chi(Q,\omega)$ in the superfluid phase has two components, a *single-particle* (or single-quasiparticle) part G described by the single-particle Green function, whose weight depends directly on the *condensate fraction* n_0, and a second part (χ_R) related to the *non-condensate* atoms. In this formulation the low-Q

'phonon' peak, which seems to remain relatively well defined at all temperatures both below and above T_λ, is identified with a *collective density (zero-sound) mode* as observed in other liquids such as Ne (Bell *et al* 1973) and in liquid ^{3}He (Scherm *et al* 1987). The existence of this excitation mode is a consequence of the strong interatomic interactions, which are not expected to be strongly temperature dependent. This mode is expected to broaden with increasing wavevector and by about 0.5 Å^{-1} it has broadened to the extent that it can no longer be seen as a well defined *collective* zero-sound mode. In the maxon–roton wavevector region it remains only as a broad intensity distribution with the sharp phonon–maxon–roton peak arising from *single-particle excitations*. The essence of the GG model is then that $\chi(Q,\omega)$ splits naturally into two components: the first term involves the excitation of a single quasiparticle out of the condensate and so has zero weight above T_λ while the second term describes the coherent density excitations of a cold quantum liquid, independent of the condensate. For more details of the theoretical justification of this model and of its description of the experimental $S(Q,\omega)$ the reader is referred to the original articles cited above.

Many of the qualitative features predicted by this model can be seen in the data of Andersen *et al* (1994). The low-Q phonon peak broadens but remains at essentially the same energy well into the normal fluid phase. Both the maxon and roton excitations decrease very rapidly in strength as T_λ is approached, leaving a very broad intensity distribution, peaked at a significantly different energy, in the normal phase. At wavevectors above about 0.5 Å^{-1}, the GG interpretation describes a sharp peak arising from single-particle excitations, which disappears at T_λ, leaving only a broad density mode. This picture is in qualitative agreement with the data of paper I, where the sharp peak present at low temperature is seen to disappear at T_λ.

Glyde (1992) and Griffin (1993) have developed separate parametrizations of the GG model. Glyde (1992) has calculated lineshapes of $S(Q,\omega)$ as a function of temperature, with parameters taken from neutron scattering data, which demonstrate the qualitative temperature dependence which can be expected from the GG scenario. The details of the parametrization are beyond the scope of the present paper, but the parameters used to calculate the GG $S(Q,\omega)$ are essentially as given in table II of Glyde (1992). Figure 9 compares these calculations with the experimental data for $Q = 0.40$, 1.1, and 1.95 Å^{-1}. At the phonon wavevector the model scattering function reproduces reasonably well the rapid change in strength in the superfluid phase and the relatively small changes that occur on passing the lambda point. For the maxon the more dramatic effects close to T_λ are apparent in both data and model; the calculation reproduces the shift of intensity from the broad density mode to the sharp quasiparticle excitation as the temperature is lowered. However, the calculation significantly overestimates the scattering intensity on the low-energy side of the one-phonon peak. While the data at low temperature show a sharp symmetric peak with no additional intensity at energies below the peak, the calculation gives a strongly asymmetric peak with significant intensity at low energy. On the high-energy side of the calculated maxon peak we see an increasing dip as the temperature is lowered, known as 'hole burning', which seems to occur in the data as well. However, the data also show a marked decrease in intensity on the low-energy side of the peak, while in the calculated lineshape the intensity in this region actually increases with decreasing temperature.

At the roton wavevector both model and data concentrate the strength into a very sharp symmetric (quasiparticle) peak. Intensity is transferred progressively to the lower-energy broad density excitation as the temperature increases. However, the data show a clear increase with temperature in the scattering intensity just above the roton peak, which is not reproduced by the calculation. The position of the dip in the calculation (hole burning)

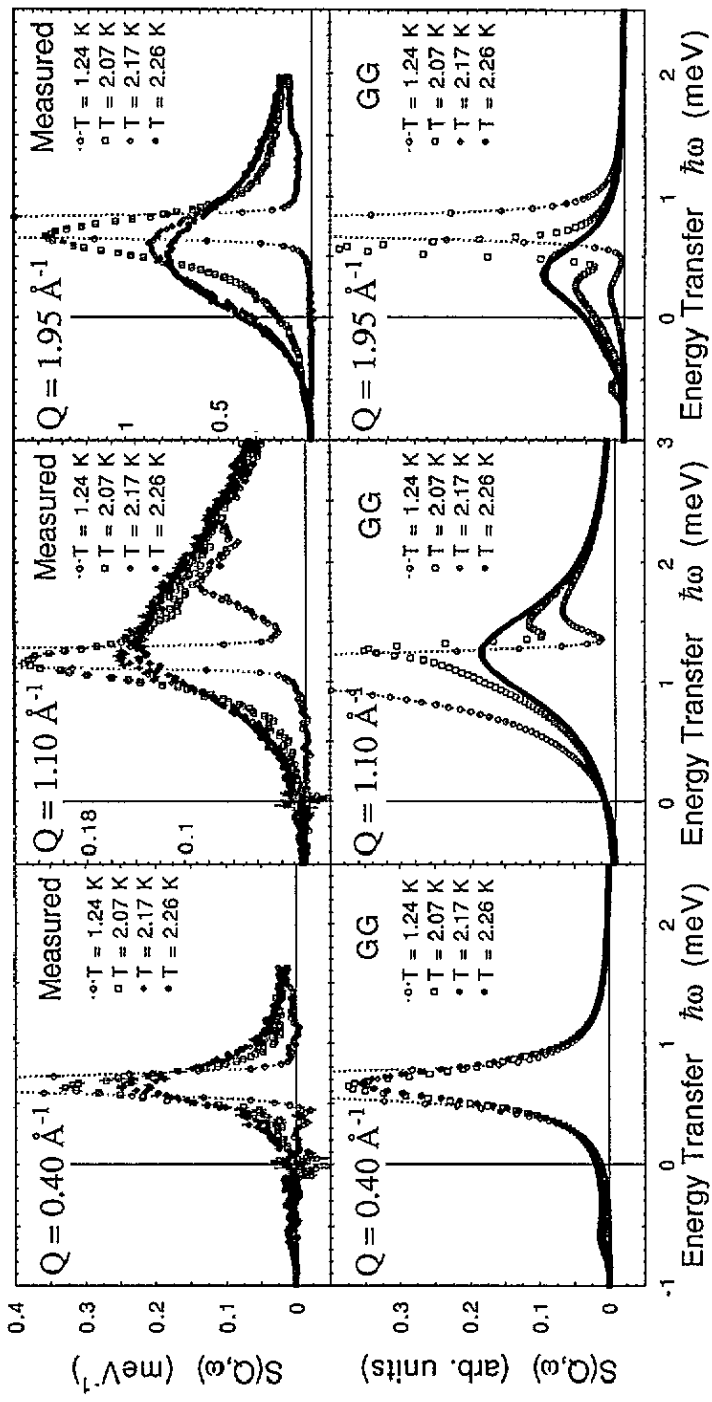

Figure 9. Comparison of measured (upper panels) and calculated (lower panels) $S(Q, \omega)$ for the representative wavevectors of figure 5 for temperatures below and near T_λ. The calculations represent the parametrization (Glyde 1992) of the GG model discussed in the text. The calculated lineshape has been convoluted with the best-fit resolution function (equation (3)) for comparison with the experimental data.

has switched from being above the one-phonon peak at the maxon to below at the roton, which means that there is no mechanism in the present GG parametrization to decrease the intensity on the high-energy side of the roton peak as the temperature is lowered. The calculated lineshape also seems to imply that $S(Q)$, the integrated scattering intensity, at the roton should change dramatically at T_λ, while measurements (Glyde and Svensson 1987) show that $S(Q)$ at the roton is approximately independent of temperature. The loss of intensity in the sharp peak as the temperature increases is not adequately compensated for by the broad density excitation mode. As in the maxon case, the model underestimates the scattering intensity at high energies, since multiphonon effects have not been included in the calculation.

To summarize, there are seen to be significant discrepancies between the data of paper I and the calculated GG lineshapes. The present parametrization, however, includes some important simplifications, which are not inherent in the GG model itself. The main simplification in the temperature dependence lies in assuming that all the parameters describing the lineshape, except n_0 the condensate fraction, are independent of temperature. Our aim was to show that even using this simple parametrization, the GG model (i) is able to reproduce the observed temperature variation of the one-phonon peak, which goes from being the dominant feature at low temperature to disappearing at T_λ and (ii) can show the correct qualitatively different temperature dependences in the phonon and maxon–roton regions. This is exemplified by figure 9.

A large part of the discrepancy between the observed and calculated lineshapes may arise from the assumed shape and temperature dependence of the broad density excitation (zero-sound) mode. The present parametrization has used a DHO lineshape to describe this mode at all wavevectors. However, when the excitation is very broad, which occurs at $Q \gtrsim 0.5$ Å^{-1}, it cannot be well described in terms of a simple energy and lifetime picture. A way of correcting for this would be to introduce an energy and temperature dependence into the half width Γ_0 of the zero-sound mode. There are good reasons to expect Γ_0 to increase with increasing temperature in the low-frequency region; these will be summarized briefly. At low temperatures the lifetime of the zero-sound mode and hence $\Gamma_0(\omega)$ is given mainly by the three-phonon decay process, the decay of a single phonon into two others (see, for example, Maris 1977, Mezei and Stirling 1983). Kinematic considerations restrict the effect of three-phonon processes to small wavevectors or high energies. At higher temperatures, however, the width $\Gamma_0(\omega)$ is dominated by four-phonon processes, which require the presence of a thermally excited phonon. Hence as the temperature is decreased the width of the zero-sound mode will decrease as the number of thermally excited phonons available for the four-phonon decay process decreases. This effect will be strongest at frequencies below the sharp maxon–roton excitation. Another reason for expecting the width to decrease with decreasing temperature is the condensate-induced coupling with Γ_{SP}, the width of the single quasiparticle peak in the GG picture (Glyde 1992). This effect is strongest at low Q where the coupling is such that the zero-sound mode and the single quasiparticle peaks are coupled into a single peak. Though the coupling strength decreases with Q it will still be significant in the maxon–roton region, but this has been neglected in the present GG parametrization for the sake of simplicity.

Examination of figure 9 shows that it is the lack of temperature dependence at low energy in the broad density mode that gives rise to the main discrepancies between the calculated lineshape and our data. A Γ_0 which decreases at low energy as the temperature is lowered would deplete intensity in the zero-sound mode around the sharp quasiparticle peak. This would remove the excess intensity below the sharp peak at low temperature in the maxon region. In the roton region it would provide a mechanism to reduce the intensity

on the high-energy side of the one-phonon peak as the temperature is decreased, allowing the high-temperature zero-sound mode to be given more intensity, in better agreement with our data.

7. Discussion and conclusion

We have analysed the new measurements by Andersen *et al* (1994) of $S(Q,\omega)$ of liquid ^{4}He covering wavevectors from 0.3 to 2.1 Å^{-1} and temperatures from 1.24 to 4.95 K. In the superfluid phase parameters have been extracted to investigate the temperature dependence of the one-phonon peak. For this purpose, two different procedures were employed, the Woods–Svensson (WS) decomposition, and a simple subtraction (SS) of the multiphonon spectrum. The one-phonon parameters are found to depend sensitively on the analysis method used, particularly near T_λ. Although it provides a good qualitative representation, the WS decomposition does not describe the observed temperature dependence accurately. A WS decomposition with the normal and superfluid parts scaling non-linearly with ρ_N and ρ_S may succeed in describing the temperature dependence well, but this involves the introduction of yet another free parameter in the fits and is no more physically meaningful than the original WS model. Separating $S(Q,\omega)$ into condensate and non-condensate parts is intuitively appealing, in particular at the maxon and roton wavevectors, where the sharp peak is seen to disappear at T_λ. However, at low Q, where the scattering does not obviously split into two components and remains reasonably well defined at all temperatures, such a decomposition does not seem necessary. The assumption that the temperature dependence of $S(Q,\omega)$ is qualitatively the same at all wavevectors is oversimplistic.

The SS procedure is useful in that it allows the extraction of one-phonon parameters at all temperatures. The method does not implicitly assume any qualitative change upon going through T_λ as does the WS procedure. It is thus significant that the energy, width and intensity of the SS one-phonon peaks change significantly at or just below T_λ. This can be understood in terms of the model proposed by Glyde and Griffin (GG), which explains the observed $S(Q,\omega)$ as containing contributions from both single-particle and zero-sound (density) excitations, the former of which is weighted by the condensate fraction n_0. Glyde (1992) argues that the strong coupling between the zero-sound mode and the single-particle excitations means that they share the same pole in the density fluctuation spectrum at low Q. This implies that at low Q, the peak in $S(Q,\omega)$ contains contributions from both types of excitation, one of which disappears at T_λ. The observed energy shift at T_λ (figure 6) may be due to the decoupling of the two modes as the condensate fraction goes to zero.

The data are compared with a parametrization of the GG model due to Glyde (1992), which successfully reproduces the rapid temperature variation of the one-phonon peak. The present GG parametrization also shows correctly how $S(Q,\omega)$ changes very rapidly with temperature just below T_λ and only very slowly above T_λ. The main discrepancies between the data and the calculated GG lineshapes appear to arise from the assumption that the zero-sound mode is independent of temperature, which is not expected to be an accurate description, especially at low energies. Thus the problems seem to arise from the parametrization and are not inherent in the GG model. Figure 9 shows that it is possible with the present GG parametrization to reproduce the observed data reasonably well. The introduction of an energy and temperature dependence into the width Γ_0 of the broad zero-sound mode may improve the agreement further. However, all the parameter values used in the calculation have been taken from neutron scattering data. It would be interesting to see whether these parameter values as well as the implied temperature variation of Γ_0 are

consistent with other theories and thermodynamic data. The agreement with the present data shows that the GG scenario is capable of producing roughly the correct lineshapes, but an evaluation of the parameters from sources other than $S(Q,\omega)$ would provide an important test of the GG picture.

The WS idea of separating $S(Q,\omega)$ into condensate and non-condensate parts is to some extent reinforced by the GG formalism. In this formulation the irreducible susceptibility χ, as used in the dielectric formalism, does indeed consist of condensate and non-condensate parts, though there are important differences between this and the WS model. The condensate term in χ, though it does go to zero at $T > T_\lambda$, does not necessarily scale as ρ_S, but as a rather complicated function of n_0. The non-condensate term does not scale as ρ_N, but is, to a first approximation, independent of temperature. Moreover, when deriving an expression for the dynamic susceptibility based on the irreducible χ, GG find that the condensate and non-condensate terms become strongly coupled, which means that $S(Q,\omega)$ cannot be expected to decompose simply into additive condensate and non-condensate components in the same way as χ does. It is interesting to note that the WS decomposition does succeed in describing the temperature dependence rather well by letting the broad component scale as ρ_N. It appears in fact that the main disagreements between our data and the calculated GG lineshapes would be removed if the non-condensate component did, in some way, go to zero at low temperature. This is the kind of temperature dependence one would hope to find arising from a temperature and energy dependent Γ_0 in a more detailed parametrization of the GG model.

Acknowledgments

The authors are grateful to the Institut Laue–Langevin for the provision of the neutron scattering facilities used in this work. KHA acknowledges the award of an ILL studentship and a fellowship from the Japan Society for the Promotion of Science. We particularly thank H R Glyde and B Fåk for many stimulating discussions and for a critical reading of the manuscript. The advice of A Griffin and R Scherm is gratefully acknowledged. Financial support was provided by the UK Science and Engineering Research Council, by the North Atlantic Treaty Organisation, and by Keele University.

References

Andersen K H, Stirling W G, Scherm R, Stunault A, Fåk B, Godfrin H and Dianoux A J 1992 *Physica* B **180 & 181** 851

—— 1994 *J. Phys.: Condens. Matter* **6** 821

Bedell K, Pines D and Zawadowski A 1984 *Phys. Rev.* B **29** 102

Bell H G, Kollmar A, Allifeld B and Springer T 1973 *Phys. Lett.* **45A** 479

Cowley R A and Woods A D B 1971 *Can. J. Phys.* **49** 177

Donnelly R J, Donnelly J A and Hills R N 1981 *J. Low Temp. Phys.* **44** 471

Dorner B 1992 *Physica* B **180 & 181** 261

Gavoret J and Nozieres P 1964 *Ann. Phys., NY* **28** 349

Glyde H R 1992 *Phys. Rev.* B **45** 7321

Glyde H R and Griffin A 1990 *Phys. Rev. Lett.* **65** 1454

Glyde H R and Svensson E C 1987 *Methods of Experimental Physics* vol 23, ed D L Price and K Skold (New York: Academic) Pt B, p 303

Griffin A 1993 *Excitations in a Bose-condensed Liquid* (Cambridge: Cambridge University Press)

Hugenholtz N and Pines D 1959 *Phys. Rev.* **116** 489

Landau L D and Khalatnikov I M 1949 *Zh. Eksp. Teor. Fiz.* **19** 637

Maris H J 1977 *Rev. Mod. Phys.* **49** 341
Marshall W G 1994 *Thesis* Birkbeck College, University of London
Maynard J 1976 *Phys. Rev.* B **14** 3868
Mezei F 1980 *Phys. Rev. Lett.* **44** 1601
Mezei F and Stirling W G 1983 *75th Jubilee Conf. on Helium-4 (St Andrews, 1983)* ed J G M Armitage (Singapore: World Scientific) p 111
Miller A, Pines D and Nozieres P 1962 *Phys. Rev.* **127** 1452
Minéev V P 1980 *JETP Lett.* **32** 489
Palevsky H, Otnes K, Larsson K E, Pauli R and Stedman R 1957 *Phys. Rev.* **108** 1346
Scherm R, Guckelsberger K, Fåk B, Sköld K, Dianoux A J, Godfrin H and Stirling W G 1987 *Phys. Rev. Lett.* **59** 217 and references therein
Stirling W G 1991 *Excitations in Two-dimensional and Three-dimensional Quantum Fluids* ed A G F Wyatt and H J Lauter (New York: Plenum) p 25
Stirling W G and Glyde H R 1990 *Phys. Rev.* B **41** 4224
Talbot E F, Glyde H R, Stirling W G and Svensson E C 1988 *Phys. Rev.* B **38** 11 229
Woods A D B, Hilton P A, Scherm R and Stirling W G 1977 *J. Phys. C: Solid State Phys.* **10** L45
Woods A D B and Svensson E C 1978 *Phys. Rev. Lett.* **41** 974